NATIONAL ADVISORY COMMITTEE FOR AERONAUTICS

WARTIME REPORT

ORIGINALLY ISSUED

April 1945 as
Advance Restricted Report 5A11

AN INVESTIGATION OF AIRCRAFT HEATERS

XXII - MEASURED AND PREDICTED PERFORMANCE OF A FLUTED-TYPE EXHAUST GAS AND AIR HEAT EXCHANGER

By L. M. K. Boelter, A. G. Guibert, J. M. Rademacher,
and F. E. Romie
University of California

NACA

WASHINGTON

NACA ARR No. 5A11

NATIONAL ADVISORY COMMITTEE FOR AERONAUTICS

ADVANCE RESTRICTED REPORT

AN INVESTIGATION OF AIRCRAFT HEATERS

XXII - MEASURED AND PREDICTED PERFORMANCE OF A FLUTED-TYPE EXHAUST GAS AND AIR HEAT EXCHANGER

By L. M. K. Boelter, A. G. Guibert, J. M. Rademacher, and F. E. Romie

SUMMARY

Data on the thermal performance and the static and total pressure drop characteristics of a fluted-type exhaust gas and air heat exchanger are presented. A shroud which produced parallel flow of the fluids was used in these tests.

The weight rates of exhaust gas through the heat exchanger were varied from 1900 to 5200 pounds per hour and the weight rates of ventilating air were varied from 1500 to 4600 pounds per hour. The inlet temperature of the exhaust gas was maintained at approximately 1600° F.

Total pressure traverses and static pressure measurements were recorded at several points upstream and downstream from the heater section in the ventilating air side of the unit under isothermal and non-isothermal conditions. Over-all isothermal and non-isothermal static pressure drops were measured across the exhaust gas and ventilating air sides of the experimental heater-duct system.

The measured thermal outputs and pressure drops are compared with predicted magnitudes.

INTRODUCTION

The performance characteristics of this fluted-type heat exchanger, designed for use in the exhaust gas streams of aircraft engines for cabin heating systems and for wing- and

tail-surface anti-icing systems, were investigated, using the large test stand of the Mechanical Engineering Laboratories of the University of California.

The following data were obtained:

1. Weight rates of the exhaust gas and ventilating air through the respective sides of the heat exchanger

2. Temperatures of the exhaust gas and ventilating air at inlet and outlet of the exchanger

3. Over-all static pressure drops (isothermal and non-isothermal) across the exhaust gas side of the heat exchanger and also across the ventilating air side of the heat exchanger both when the air flowed out of the "cabin-air" duct and also when the air flowed out of the "overboard" duct. (See fig. 1.) Also, static pressure measurements under isothermal and non-isothermal conditions were taken at six points arranged around the periphery of the shroud, three at the upstream end, and three at the downstream end of the heater section. The isothermal static pressure drop on the exhaust gas side across the heat exchanger alone was also measured.

4. Total pressure traverses on the ventilating air side at seven points on the periphery of the shroud; three of these being traverses at the upstream end of the heater section, three at the downstream end, and one in the center of the heater section within one of the air side flutes. An eighth total pressure traverse was made on the ventilating air side across that exit duct which conveys the cabin air. These total pressure traverses were made under isothermal and non-isothermal conditions.

This investigation, part of a research program conducted on aircraft heat exchangers at the University of California, was sponsored by and conducted with the financial assistance of the National Advisory Committee for Aeronautics.

SYMBOLS

A	area of heat transfer, ft^2
A_h	cross-sectional area of flow for either fluid measured within the heater, ft^2
A_1	cross-sectional area of flow taken at the inlet pressure measuring station, ft^2
A_2	cross-sectional area of flow taken at the outlet pressure measuring station, ft^2
c_p	heat capacity of the fluid at constant pressure, Btu/lb ^oF
D	hydraulic diameter, ft
f_c	unit thermal convective conductance (average with length), Btu/hr ft^2 ^oF
f_cA	thermal conductance of either fluid, Btu/hr ^oF
ΔF_{iso}	isothermal frictional pressure loss across the heater section at temperature T_{iso}, lb/ft^2
g	gravitational force per unit of mass, $lb/(lb\ sec^2/ft)$
G	weight rate of fluid per unit of area, lb/hr ft^2
K	isothermal head loss coefficient defined by the equation $\frac{\Delta P}{\gamma} = K \frac{u_m^2}{2g}$
l	length of a duct measured from the entrance, ft
m	ratio of the cross-sectional area of flow before expansion of the fluid passage to that after expansion of the fluid passage
q	measured rate of enthalpy change of the fluid, Btu/hr or k Btu/hr (k Btu designates kilo Btu, or 1000 Btu/hr)
T_{av}	arithmetic average mixed-mean absolute temperature of fluid $= \frac{T_1 + T_2}{2}$, ^oR

T_{iso} mixed-mean absolute temperature of fluid for the isothermal pressure drop tests, ^{o}R

T mixed-mean absolute temperature of the fluid, ^{o}R

u_m mean velocity of fluid within the fluid passage, ft/sec

U over-all unit thermal conductance, Btu/hr ft^2 ^{o}F

UA over-all thermal conductance, Btu/hr ^{o}F

W weight rate of fluid, lb/hr

Re Reynolds number = $3D/3600\,\mu g$

γ weight density of fluid, lb/ft^3

ΔP static pressure drop, lb/ft^2

ΔP_{total} total pressure drop, lb/ft^2

$\Delta P''$ pressure drop, inches of water

ζ isothermal friction factor defined by the equation

$$\frac{\Delta P_{fric}}{\gamma} = \zeta \cdot \frac{l}{D} \frac{u_m^2}{2g}$$

μ viscosity of the fluid, lb sec/ft^2

τ mixed-mean temperature of the fluid, ^{o}F

φ_p heater effectiveness for parallel flow of fluids. This effectiveness is defined by the equation

$$q_a = W_a c_{p_a} (\tau_{g_1} - \tau_{a_1}) \varphi_p$$

Subscripts

a ventilating air side

c convective conductance (f_c, etc.) and also sudden contraction (K_c)

e sudden expansion

g the exhaust gas side

h heater

m mean values at any section of the heater (u_m)

p parallel flow

av arithmetic average

contr sudden contraction

gr contr gradual contraction

gr exp gradual expansion

fric friction

iso isothermal conditions

non-iso non-isothermal conditions

1 point 1, entrance of section of heater

2 point 2, exit of section of heater

DESCRIPTION OF HEATER AND TESTING PROCEDURES

The fluted-type heat exchanger tested was a parallel flow unit with 30 alternate exhaust gas and ventilating air passages. (See fig. 1.) It was similar in design to the fluted-type heat exchangers tested previously and reported in references 1 and 2.

The ventilating air shroud used (see fig. 1) was a design for an actual aircraft installation. It produced parallel flow of fluids along the heater section. There were two exit ducts for the ventilating air. One, termed the overboard duct, conducted some of the ventilating air away from the heater section and the other duct, termed the cabin-air duct, conveyed the remainder. Only one of these exits was used at any one time during the tests.

The static pressure drops across the test setup (entrance ducts, heater, exit ducts) were measured on each side of the heat exchanger by means of wall taps at the inlet and outlet ends of the entrance and exit ducts. Static pressure drops were also measured across the heater section on the ventilating air side by means of special "button" taps which were

inserted at three points on the periphery of the shroud at the entrance to the heater section and at another three points at the exit to the heater section. The readings obtained with these button taps were compared with those obtained using ordinary wall taps and, for the range of weight rates per unit of area employed in these tests, they were found to be about 1 to 3 percent lower than those obtained with the wall taps. The error involved in the measurement of a pressure drop probably would be smaller, because the velocities at the two pressure-measuring stations are approximately the same.

Total pressure measurements were taken at the same sections of the shroud where the static pressures were measured. Shielded total pressure tubes, which gave constant readings even when the angle of the total pressure tube with respect to the direction of flow varied up to approximately 60°, were used for the measurements.

All pressure drop measurements were made under isothermal and non-isothermal conditions, except for the static pressure drop across the exhaust gas side of the heat exchanger alone, which was taken under isothermal conditions only.

METHOD OF ANALYSIS

Heat Transfer

The evaluation of the thermal output of the heat exchanger and duct system was based upon the enthalpy change of the ventilating air as given by the equation:

$$q_a = W_a c_{p_a} (T_{a_2} - T_{a_1}) \qquad (1)$$

in which c_{p_a}, the heat capacity of the air, was evaluated at the arithmetic average ventilating air temperature. Figure 2 presents a plot of q_a as a function of W_a at constant values of the exhaust gas rate W_g.

For the ideal case of a heat exchanger thermally insulated from its surroundings, the enthalpy change of the exhaust gas,

$$q_g = W_g c_{p_g} (T_{g_1} - T_{g_2})^* \qquad (2)$$

*The heat capacity of the exhaust gas c_{p_g} is taken as that of air at the average exhaust gas temperature.

would be equal to the enthalpy change of the ventilating air q_a. However, because the heat balance ratios q_g/q_a (see table I) indicate that the enthalpy changes are not equal in the actual case, and because experience has shown that q_a is the more reliable value, the enthalpy change of the ventilating air q_a is chosen as the value for the heat transfer rate.

The prediction of the thermal output of the unit was attempted. It must be stated that the thermal output determined experimentally was not that of the heater alone but that of the heater and those sections of the exhaust gas ducts which were covered by the ventilating air shroud. Because it would have been difficult to measure separately the contribution of each section to the heat transfer, only the sum of these contributions was measured.

The predictions of the heat transfer rate are based upon the division of the heater-duct system into three sections and the summation of the thermal output of each section in order to obtain the total heat transfer rate. The comparison of measured and predicted values of the over-all thermal conductance UA, which is the quotient of the total heat transfer rate divided by a mean temperature difference, is not made in this report because the over-all unit thermal conductance U varied greatly in the three sections of the heater. The over-all thermal conductance, if calculated, would then be some mean of those which obtained over the individual sections and would be only an approximation in evaluating the performance of the unit for other inlet temperature conditions.

For the prediction of the thermal output it was necessary to apply a step-by-step calculation at each section because only the temperatures at the entrance to the first section of the heater system (and the weight rates of the fluids) were known. The calculation began with an estimation of the temperatures at the exit of the approach section, in order to estimate the mean temperatures of the fluids. These are needed for the calculation of the unit thermal convective conductances of the two fluids within the approach section. The equation used to determine the unit thermal convective conductances for the ventilating air and exhaust gas at any section was

$$f_c = 5.4 \times 10^{-4} (T_{av})^{0.3} \frac{G^{0.8}}{D^{0.2}} \left(1 + 1.1 \frac{D}{l}\right) \qquad (3)$$

where

T_{av} estimated arithmetic average temperature of fluid

G weight rate of fluid per unit cross-sectional area

D hydraulic diameter of passage

l length of passage

The unit thermal conductances calculated in this manner include the "entrance effect" correction factor $1 + 1.1\ D/l$, which is used to account for the higher values of the unit thermal conductances along the entrance length of a heat transfer surface before the boundary layer completely fills the passages. (See reference 2.)

From the unit thermal conductances and the heat transfer areas, the over-all thermal conductance for each individual section was calculated according to the equation:

$$UA = \frac{1}{\left(\frac{1}{f_c A}\right)_a + \left(\frac{1}{f_c A}\right)_g} \tag{4}$$

(See reference 3, equation (46).) From these over-all thermal conductances and the inlet temperature conditions, the thermal output of each section was computed. The equation employed was

$$q = W_a\ c_{p_a}\ (T_{g_1} - T_{a_1})\ \varphi_p \tag{5}$$

where

W_a weight rate of ventilating air

c_{p_a} heat capacity of ventilating air

T_{g_1} inlet temperature of exhaust gas at that section

T_{a_1} inlet temperature of ventilating air at that section

φ_p heater effectiveness for parallel flow (a function of UA, $W_a\ c_{p_a}$, and $W_g\ c_{p_g}$)

The value of the heater effectiveness φ_p was obtained from a plot of φ_p as a function of the ratio $W_a\ c_{p_a}/W_g\ c_{p_g}$, using $UA/W_a\ c_{p_a}$ as a parameter. (See reference 3, fig. 32.) The equation:

$$\varphi_p = \frac{1 - e^{-(1 + W_a\ c_{p_a}/W_g\ c_{p_g})(UA/W_a\ c_{p_a})}}{1 + W_a\ c_{p_a}/W_g\ c_{p_g}} \qquad (6)$$

which is the basis for the plot mentioned above, is derived in reference 4. By using the value of φ_p calculated, the exit temperatures postulated for the approach section were checked. If the agreement was satisfactory, the exit temperatures corresponding to the φ_p calculated were used as the inlet temperatures for the heater section. Fluid temperatures at the exit of the heater section were postulated to find the mean temperature of each of the fluids in that section and the process of calculation was repeated for the heater section. The same procedure was applied to the exit section to complete the calculations. The predicted thermal output of the unit was then obtained by summation of the thermal outputs predicted for each section.

SAMPLE CALCULATIONS

Compute the thermal performance of the heat exchanger-duct system for the following conditions:

$T_{a_1} = 95^\circ$ F $= 555^\circ$ R $\qquad W_a = 3000$ lb/hr

$T_{g_1} = 1600^\circ$ F $= 2060^\circ$ R $\qquad W_g = 3050$ lb/hr

Only the computation of the thermal performance of the entrance section is given here, since the others are entirely similar, all of them being based on the equation:

$$q_a = W_a\ c_{p_a}\ (T_{g_1} - T_{a_1})\ \varphi_p$$

where the subscripts 1 refer to the conditions at the inlet of the section under consideration.

Determine φ_p for the entrance section.

Unit thermal convective conductances determined from the equation:

$$f_c = 5.4 \times 10^{-4} T_{av}^{0.3} \frac{G^{0.8}}{D^{0.2}} \left(1 + 1.1 \frac{D}{l}\right)$$

a. For the exhaust gas side:

Flow area = 0.217 ft^2

$$G = \frac{W}{A} = \frac{3050}{0.217} = 14,000 \text{ lb/hr ft}^2$$

D = 0.526 ft

Correction $(1 + 1.1\ D/l)$ is not applied because a new boundary layer is not formed here. Estimated temperature of exhaust gas at outlet of entrance section:

1540° F = 2000° R

$$T_{av} = \frac{2000 + 2060}{2} = 2030^\circ \text{ R}$$

$$f_c = 5.4 \times 10^{-4} (2030)^{0.3} \frac{(14\,000)^{0.8}}{(0.526)^{0.2}}$$

$$= 5.4 \times 10^{-4} \times 9.84 \times \frac{2080}{0.819}$$

f_c = 12.6 Btu/hr ft^2 $^\circ$F

Heat transfer area = 3.87 ft^2

$f_c A$ = 12.6 x 3.87 = 48.6 Btu/hr $^\circ$F

b. For the ventilating air side

Flow area = 0.254 ft^2

$$G = \frac{W}{A} = \frac{3000}{0.254} = 11,800 \text{ lb/hr ft}^2$$

D = 0.222 ft

$1 + 1.1\ D/l$ correction is not applied.

Postulate temperature of ventilating air at outlet of entrance section = 145° F = 605° R

$$T_{av} = \frac{555 + 605}{2} = 580^\circ \text{ R}$$

$$f_c = 5.4 \times 10^{-4} (580)^{0.3} \frac{(11800)^{0.8}}{(0.222)^{0.2}} = 5.4 \times 10^{-4} \times 6.74 \times \frac{1810}{0.740}$$

$$= 8.94 \text{ Btu/hr ft}^2 \text{ °F}$$

Heat transfer area = 3.87 ft^2

$$f_c A = 8.94 \times 3.87 = 34.7 \text{ Btu/hr °F}$$

The over-all thermal conductance:

$$UA = \frac{1}{\left(\frac{1}{f_c A}\right)_a + \left(\frac{1}{f_c A}\right)_g}$$

$$= \frac{1}{\frac{1}{48.6} + \frac{1}{34.7}} = \frac{1}{0.0206 + 0.0388} = \frac{1}{0.0494} = 20.2 \text{ Btu/hr °F}$$

Find φ_p from chart, figure 32 of reference 3.

$$\frac{W_a c_{p_a}}{W_g c_{p_g}} = \frac{3000 \times 0.242}{3050 \times 0.278} = 0.857$$

$$\frac{UA}{W_a c_{p_a}} = \frac{20.2}{3000 \times 0.242} = 0.0279$$

If the preceding values are inserted into the chart referred to, there is obtained

$$\varphi_p = 0.026$$

Therefore, the thermal performance of the entrance section is:

$$q = W_a c_{p_a} (T_{g_1} - T_{a_1}) \varphi_p = 3000 \times 0.242 \times 1505 \times 0.026$$

$$= 28,400 \text{ Btu/hr}$$

From the relationships:

$$q = W_a c_{p_a} (T_{a_2} - T_{a_1}) = W_g c_{p_g} (T_{g_1} - T_{g_2})$$

$$T_{a_2} = 135^\circ \text{ F}$$

$$T_{g_2} = 1566^\circ \text{ F}$$

These values agree sufficiently well with the exit temperatures estimated for the above calculation.

The preceding temperatures are the inlet temperatures of the heater section. If fluid temperatures at the outlet of the heater section are postulated, the thermal performance of that section is calculated and then, in turn, the thermal performance of the exit section is obtained. The results of the calculations are:

	T_a(in) ($^\circ$F)	T_a(out) ($^\circ$F)	T_g(in) ($^\circ$F)	T_g(out) ($^\circ$F)	f_{c_a} $\left(\frac{\text{Btu/hr}}{\text{ft}^2\ ^\circ\text{F}}\right)$	f_{c_g} $\left(\frac{\text{Btu/hr}}{\text{ft}^2\ ^\circ\text{F}}\right)$	UA (Btu/hr$^\circ$F)	φ_p	q_a (kBtu/hr)
Entrance section	95	135	1600	1566	8.94	12.6	20.2	0.026	28.4
Heater section	135	331	1566	1393	15.7	16.2	117	.134	139
Exit section	331	352	1393	1374	6.38	11.6	12.8	.0176	13.6

Thermal performance of heater-duct system:

$$q_a = 28,400 + 139,000 + 13,600 = 181,000 \text{ Btu/hr}$$

Experimental value (interpolated from plot of q_a vs W_a in fig. 2):

$$q_a = 220,000 \text{ Btu/hr}$$

Percentage deviation = 18 percent

PRESSURE DROP

Isothermal Pressure Drop

The isothermal static pressure drop on the exhaust gas side of the heater section alone was measured experimentally. The predicted pressure drop was based upon the following partially idealized system:

(a) Static pressure drop in a converging adapter from the upstream pressure measuring section to the heater, as given by the equation:

$$\frac{\Delta P_{gr\ contr}}{\gamma} = K_{gr\ contr}\frac{u_m^2}{2g} \quad (K_{gr\ contr} = 0.04) \qquad (7)$$

where u_m is the mean velocity of flow at the heater end of the adapter, and $K_{gr\ contr}$ is a "head loss" coefficient for gradual contraction of the air obtained from reference 5.

(b) Static pressure drop due to a sudden contraction in the area of flow as the gas enters the fluted section of the heater, given by the equation:

$$\frac{\Delta P_{contr}}{\gamma} = K_c\frac{u_m^2}{2g} \quad (K_c = 0.02) \qquad (8)$$

where u_m is the mean velocity in the fluted section of the heater and K_c is a head loss coefficient for sudden contraction, obtained from reference 5.

(c) Static pressure drop due to friction losses within the fluted section of the heater, given by the equation:

$$\frac{\Delta P_{fric}}{\gamma} = \zeta\frac{l}{D}\frac{u_m^2}{2g} \qquad (9)$$

where u_m is evaluated for the area of the fluted section and ζ is the friction factor for commercial pipe, obtained from reference 6.

(d) Static pressure drop due to a sudden expansion in the area of flow as the gas leaves the fluted section of the heater, given by the equation:

$$\frac{\Delta P_{exp}}{\gamma} = K_e \frac{u_m^2}{2g} \quad (K_e = 0.011) \tag{10}$$

where u_m is evaluated for the area of the fluted section of the heater and K_e is a head loss coefficient for sudden expansion, equal to $(1 - m)^2$ where m is the ratio of the two areas of flow.

(e) Static pressure drop due to sudden contraction in the area of flow as the heater end changes from a circle to an ellipse of smaller area, given by the equation:

$$\frac{\Delta P_{contr}}{\gamma} = K_c \frac{u_m^2}{2g} \quad (K_c = 0.13) \tag{11}$$

where u_m is evaluated for the area of the ellipse and K_c is determined, as before, from reference 5.

(f) Static pressure drop due to gradual expansion of the flow area from the elliptical heater end to the circular pressure measuring section, given by the equation,

$$\frac{\Delta P_{gr\ exp}}{\gamma} = K_{gr\ exp} \frac{u_m^2}{2g} \quad (K_{gr\ exp} = 0.097) \tag{12}$$

where u_m is evaluated for the flow area at the elliptical end of the heater and $K_{gr\ exp.}$ is a head loss coefficient for gradual expansion, equal to $(1 - n)(1 - m^2)$ where m is the ratio of the flow area before expansion to that after expansion, and $(1 - n)$ is an efficiency factor which is given by figure 11 of reference 5.

The summation of the pressure drops from a, b, c, d, e, and f is then the predicted value of the static pressure drop across the heater section and the adapters used in making the isothermal tests. The predicted values (see table IV and fig. 5) were, on the average, within 25 percent of the measured values.

The isothermal static pressure drop across the heater section alone on the ventilating air side was predicted in a similar manner. However, since the measurments were actually made at the entrance and exit of the heater section, there

were only three pressure drop terms to consider: (a) a sudden contraction ($K_c = 0.16$), (b) frictional pressure drop within the fluted section of the heater, and (c) a sudden expansion ($K_e = 0.24$). The same basic equations were applied and the sum of the three terms calculated. Comparison with the measured values showed that the maximum deviation, over the range considered, was about 12 percent. The experimental data and predicted values are given in table II and are plotted as a function of the ventilating air rate in figure 3.

The isothermal total pressure drop across the heater section alone on the ventilating air side was predicted by adding the loss in velocity head to the calculated static pressure drop. These predicted values differed from the measured values by about 13 percent, on the average. Table II presents the experimental data and the predicted values of the total pressure drop across the heater section alone on the ventilating air side. A plot of the data and the predictions as a function of the ventilating air weight rate is presented in figure 4.

Non-Isothermal Pressure Drop

The non-isothermal static pressure drops across either side of the heat exchanger were predicted from the isothermal measurements, using the equation (see reference 3, equation (54)):

$$\Delta P_{(static)non\text{-}iso} = \Delta F_{iso} \left(\frac{T_{av}}{T_{iso}}\right)^{1.13} + \left(\frac{W}{3600}\right)^2 \frac{1}{2g\,\gamma_1\,A_h^2} \times \left[\left(\frac{A_h^2}{A_2^2} + 1\right)\frac{T_2}{T_1} - \left(\frac{A_h}{A_1}\right)^2 + 1\right] \quad (13)$$

in which

ΔF_{iso} isothermal frictional pressure loss across the heater section at temperature T_{iso}

T_1 mixed-mean absolute temperature of the fluid at the inlet end of the heat exchanger

T_2 mixed-mean absolute temperature of the fluid at the outlet end of the heat exchanger

T_{av} arithmetic average of T_1 and T_2

W weight rate of fluid

γ_1 weight density of the fluid, evaluated at temperature T_1

A_1 cross-sectional flow area at upstream pressure tap

A_2 cross-sectional flow area at downstream pressure tap

A_h cross-sectional area of flow within the heater

The non-isothermal static pressure drop across the exhaust gas side of the heater-duct system was predicted by considering the isothermal static pressure drop as being equal to the isothermal frictional pressure loss. This substitution is quite valid because the cross-sectional areas of flow at the upstream and downstream pressure taps were equal. (See reference 3.)

This substitution was not possible in the prediction of the non-isothermal static pressure drop across the heater section alone on the ventilating air side because the flow areas at the points where the static pressures were measured, the upstream and downstream ends of the heater section, were not equal. The term ΔF_{iso}, the isothermal friction loss, was therefore replaced by the isothermal drop in total pressure, for this case.

The measured and predicted non-isothermal static pressure drops on either side of the heater are compiled in tables III and IV, and plots of these values as functions of the weight rate of the respective fluids are given in figures 3 and 6. The predicted non-isothermal static pressure drops were, on the average, within 13 percent of the measured values.

For prediction of the non-isothermal total pressure drop across the ventilating air side of the heater section alone, the equation used was (See reference 3, equation (54a).):

$$\Delta P_{(total)non\text{-}iso} = \Delta F_{iso}\left(\frac{T_{av}}{T_{iso}}\right)^{1.13} + \left(\frac{W_a}{3600}\right)^2 \frac{1}{2g\,\gamma_1\,A_1^2}\left(\frac{T_2}{T_1} - 1\right) \qquad (14)$$

where

ΔF_{iso} isothermal friction pressure loss across the heater section at temperature T_{iso}

T_{av} arithmetic average of T_1 and T_2, the mixed-mean absolute temperatures of the ventilating air at the inlet and outlet ends of the heat exchanger, respectively

W_a weight rate of the ventilating air

γ_1 weight density of the ventilating air, evaluated at temperature T_1

A_h cross-sectional area of flow within the heater

Because of the fact that the cross-sectional areas of flow were not the same at the points at which the total pressure measurements were taken, the isothermal static pressure drop ΔP_{iso} cannot be substituted for the isothermal friction pressure loss ΔF_{iso}. For this case, the term ΔF_{iso} is replaced by the isothermal total pressure drop across the section. This equation is obtained from the previous equation (13) by transposing to the left-hand side two terms on the right-hand side which are the velocity pressures at points 1 and 2, and thus obtaining the expression for the total pressure drop.

A summary of the measured and predicted total pressure drops is given in table III and a plot of these values as a function of ventilating air weight rate is presented in figure 4. The deviation of the predicted values of the nonisothermal total pressure drop on the ventilating air side from the measured values was, on the average, within 13 percent.

DISCUSSION

The results of the tests on this fluted-type heat exchanger using the parallel-flow-type B-3 shroud are shown graphically in figures 2 to 7. These graphs are based on the data presented in tables I to V.

Heat Transfer

The predictions of the over-all thermal performance of this fluted-type heater, using the parallel-flow-type shroud were, on the average, within 18 percent of the experimental values. A more complete analysis would have included the effect of heat transfer by radiation (reference 3, pt. I, sec. G) between the heater surfaces and also by gaseous radiation (reference 7) by the exhaust gas and the heater shell.

Although surface temperatures were not measured, at high gas rates and low ventilating air rates, the heater surfaces were a light orange-red color. Computations, based on the calculations of the over-all thermal performance, gave approximately 1200° F as the temperature of the heater surface for this combination of ventilating air and exhaust gas rates. For these weight rates it is probable that the heat transfer by radiation was not negligible. A rough computation of the heat transferred from the core to the shroud by radiation, and then from the shroud to the ventilating air by convection shows that this manner of heat transfer could account for approximately 15 to 20 percent of the heat transfer, thus lowering the discrepancy between the predicted and measured values of q_a.

Another partial explanation of the discrepancy between predicted and measured values of the over-all thermal performance may be that thermal stresses which distort the heater passages will affect the performance of the heater if the thermal resistances are altered. The calculations revealed, however, that the thermal resistances were on the two sides of the surface, for the most part, of the same order of magnitude and, therefore, changes in area would have little effect upon the thermal performance unless these changes were rather pronounced.

From figure 2, it can be noted that the thermal output of the heater unit was not greatly affected by the use of the cabin air duct instead of the overboard duct as the ventilating air exit. At the maximum weight rate, the result of using the cabin air duct as the ventilating air exit was to increase the thermal output by about 15 percent above that obtained when using the overboard duct as the exit. The increase became less noticeable at lower weight rates.

Pressure Drop

The isothermal static pressure drop on the exhaust gas side of the heater section alone was not measured directly, but with the addition of a converging and a diverging adapter. The static pressure drop across the adapters could not be measured directly, but calculations indicate that it comprises about 10 percent of the measured value. The pressure drop across the heater section alone can be estimated by deducting from the measured over-all values the calculated values of the pressure drop across the adapters. From figure 5, it can be noted that though the predicted values of the static pressure drop across the heater and adapters were lower than the measured values, the slopes of the two curves were essentially similar.

The predicted curves of the isothermal static and total pressure drops across the ventilating air side of the heater section alone have slopes which are greater than those of the plotted measured values. This may be due, in part, to the fact that the idealized system across which the pressure drop was predicted may not have given sufficient weight to the effect of friction.

Three-point total pressure traverses were made within the flutes of the heater shell on the ventilating air side under isothermal and non-isothermal conditions. At all weight rates, it was found that the total pressures were highest at the bottom and center of the flute. (See table V and fig. 7.) The pressure distributions obtained are not too significant because, owing to the lack of a smaller total pressure tube, the effect of the walls was greater than is desirable.

The total pressure drop across the bend of the cabin air duct was about 60 percent of that across the heater section alone, for isothermal conditions, and about 70 percent of that for non-isothermal conditions.

Non-Isothermal Pressure Drop

The non-isothermal static pressure drop across the exhaust gas side was determined for the whole unit because it was not possible to measure the pressure drop across the heater section alone.

The predictions of the non-isothermal static and total pressure drop across the heater section alone of the

ventilating air side were within approximately 8 percent of the experimental data.

The limitations of equations (13) and (14) are discussed in reference 3. It may be stated here, though, that the errors are mainly in the correction of the expansion and contraction losses by a term $\left[\left(\frac{T_{av}}{T_{iso}}\right)^{0.13}\right]$, which should be used only to correct frictional losses, and also in the use of an average density to correct approximately for the variation of pressure drop with changes of density caused by temperature and altitude effects. However, the first of these corrections is small, and, since it usually overcorrects the entrance losses and undercorrects the exit losses (or vice-versa, depending upon whether the fluid is heating or cooling), the error introduced is minimized. The second item is only an approximation because an arithmetic average temperature is used, but again because the errors introduced at entrance and exit tend to cancel one another, the net error is not so great as it would seem upon first inspection.

CONCLUSIONS

Performance data have been taken on a flute-type heat exchanger, using a parallel-flow-type shroud, and the results compared with predicted values. The thermal performance of the heater-duct system was predicted within about 18 percent. The pressure drops (isothermal and non-isothermal, static and total) were predicted with an average deviation ranging from 8 to 25 percent. The majority of the predictions deviated from the measured pressure drops by about 12 percent.

University of California,
Berkeley, Calif., July 23, 1944.

REFERENCES

1. Boelter, L. M. K., Miller, M. A., Sharp, W. H., Morrin, E. H., Iversen, H. W., and Mason, W. E.: An Investigation of Aircraft Heaters. IX - Measured and Predicted Performance of Two Exhaust Gas-Air Heat Exchangers and an Apparatus for Evaluating Exhaust Gas-Air Heat Exchangers. NACA ARR, March 1943.

2. Boelter, L. M. K., Dennison, H. G., Guibert, A. G., and Morrin, E. H.: An Investigation of Aircraft Heaters. X - Measured and Predicted Performance of a Fluted-Type Exhaust Gas and Air Heat Exchanger. NACA ARR, March 1943.

3. Boelter, L. M. K., Martinelli, R. C., Romie, F. E., and Morrin, E. H.: An Investigation of Aircraft Heaters. XVIII - A Design Manual for Exhaust Gas and Air Heat Exchangers. NACA ARR,No. 5A06, 1945.

4. Martinelli, R. C., Morrin, E. H., and Boelter, L. M. K.: An Investigation of Aircraft Heaters. VI - Heat Transfer Equations for the Single Pass Longitudinal Exchanger. NACA ARR, Dec. 1942.

5. SAE Committee A-9 Aircraft Air Conditioning Equipment: Airplane Heating and Ventilating Equipment. Engineering Data. Aero. Inf. Rep. 2, Jan. 1, 1943.

6. Martinelli, R. C., Weinberg, E. B., Morrin, E. H., and Boelter, L. M. K.: An Investigation of Aircraft Heaters. IV - Measured and Predicted Performance of Longitudinally Finned Tubes. NACA ARR, Oct. 1942.

7. Martinelli, R. C., Morrin, E. H., and Boelter, L. M. K.: An Investigation of Aircraft Heaters. VII - Thermal Radiation from Athermanous Exhaust Gases. NACA ARR, Dec. 1942.

TABLE I EXPERIMENTAL RESULTS ON FLUTED-TYPE HEATER USING B-3 SHROUD

	AIR SIDE					EXHAUST GAS SIDE					
Run No.	T_{a_1} °F	T_{a_2} °F	ΔT_a °F	W_a lb/hr	Q_a KBtu/hr	T_{g_1} °F	T_{g_2} °F	ΔT_g °F	W_g lb/hr	Q_g KBtu/hr	Q_g/Q_a —
13	94	485	391	1520	144	1604	1343	261	1930	139	0.97
14	97	388	291	2590	182	1604	1308	296	1930	157	0.86
17	97	305	208	4490	226	1605	1227	378	1940	202	0.89
23*	90	547	457	1430	158	1604	1407	197	3050	166	1.05
15	98	535	437	1520	161	1595	1381	214	3030	179	1.11
22*	91	461	370	2200	197	1600	1403	197	3050	166	0.84
16	94	427	333	2610	210	1578	1321	257	3050	216	1.03
24*	84	390	306	3200	237	1600	1364	236	3070	200	0.84
18	96	335	239	4500	260	1582	1278	304	3070	258	0.99
25*	84	330	246	4600	274	1608	1351	257	3070	218	0.79
21	95	589	494	1500	179	1586	1424	162	5160	231	1.28
20	96	513	417	2620	264	1569	1381	188	5160	268	1.04
19	92	390	298	4510	325	1610	1364	246	5110	346	1.05

* Ventilating Air out through "Cabin-Air" elbow

TABLE II.- MEASURED AND PREDICTED ISOTHERMAL PRESSURE DROPS VENTILATING AIR SIDE

Run	W_a (lb/hr)	Static ΔP" Measured (in. H_2O)	Static ΔP" Predicted (in. H_2O)	Total ΔP" Measured (in. H_2O)	Total ΔP" Predicted (in. H_2O)
Pressure Drop across the Heater Section Alone (plotted in figs. 3, 4) (Sections A-A and B-B)					
1	1010	0.16	0.14	0.19	0.15
2	2280	.65	.67	.66	.72
3	3870	1.71	1.74	1.71	1.83
4	5940	3.75	3.94	3.16	4.27
Pressure Drop across the Heater-Duct System, Using the Overboard Duct as Ventilating Air Exit (Sections D-D and H-H)					
12	1010	0.43			
11	2250	1.53			
10	3850	4.09			
9	5510	7.80			
Pressure Drop across the Heater-Duct System, Using the Cabin-Air Duct as Ventilating Air Exit (Sections D-D and F-F)(Measurements corrected to equal areas)					
1	1010	0.51			
27	1510	.89			
2	2280	1.88			
3	3870	5.11			
26	5000	7.49			
4	5940	11.3			
Pressure Drop across the Cabin-Air Duct Elbow (plotted in fig. 7) (Sections B-B and F-F)					
27	1510			0.17	
2	2280			.44	
3	3870			1.30	
26	5000			1.71	
4	5940			2.51	

NOTE: See fig. 1 for the location of the sections.

TABLE III.- MEASURED AND PREDICTED NON-ISOTHERMAL PRESSURE DROPS VENTILATING AIR SIDE

Run	W_a (lb/hr)	Static $\Delta P''$		Total $\Delta P''$	
		Measured (in. H_2O)	Predicted (in. H_2O)	Measured (in. H_2O)	Predicted (in. H_2O)
Pressure Drop across the Heater Section Alone (plotted in figs. 3, 4) (Sections A-A and B-B)					
23	1430	0.68	0.60	0.59	0.59
22	2200	1.32	1.16	1.29	1.17
24	3200	2.00	2.01	1.84	2.00
25	4600	3.43	3.47	3.35	3.51
Pressure Drop across Heater-Duct System, Using the Overboard Duct as the Ventilating Air Exit (Sections D-D and H-H)					
13	1520	1.52			
16	2610	3.53			
19	4510	8.60			
Pressure Drop across Heater-Duct System, Using the Cabin-Air Duct as the Ventilating Air Exit (Sections D-D and F-F)					
23	1430	1.52			
22	2200	2.79			
24	3200	4.86			
25	4600	8.65			
Pressure Drop across Cabin-Air Duct Elbow (plotted in fig. 7) (Sections B-B and F-F)					
23	1430			0.37	
22	2200			.60	
24	3200			1.33	
25	4600			2.15	

NOTE: See fig. 1 for the location of the sections.

TABLE IV.- MEASURED AND PREDICTED ISOTHERMAL AND NON-ISOTHERMAL STATIC PRESSURE DROPS EXHAUST GAS SIDE

Run	W_g (lb/hr)	$\Delta P''_{iso}$		$\Delta P''_{non-iso}$	
		Measured (in. H_2O)	Predicted (in. H_2O)	Measured (in. H_2O)	Predicted (in. H_2O)
Pressure Drop across Heater Section (Sections a and b, plotted in fig. 5)					
31	2570	0.29	0.24		
32	3190	.45	.36		
33	5000	1.15	.84		
34	6500	1.95	1.39		
35	9100	3.56	2.64		
Pressure Drop across Heater-Duct System (plotted in fig. 6) (Sections E-E and G-G, see fig. 1)					
7	1700	0.51			
14	1930	.68		3.02	2.51
8	2950	1.62			
15	3030	1.68		6.96	6.37
5	5000	4.58			
19	5110	4.75		19.5	18.8
6	9000	14.9			

TABLE V.- TOTAL PRESSURE DISTRIBUTION WITHIN A FLUTE ON THE VENTILATING AIR SIDE OF THE HEAT EXCHANGER (Section C-C, see fig. 1)

Run	W_a	Total pressure (in. H_2O)		
		Point a	Point b	Point c
		Isothermal		
1	1010	0.40	0.41	0.26
2	2280	1.66	1.72	1.08
3	3870	4.53	4.88	2.98
4	5940	10.2	10.5	6.57
		Non-isothermal		
23	1430	1.44	1.18	0.88
22	2200	2.74	2.84	2.26
24	3200	4.85	4.95	4.35
25	4600	8.52	8.92	5.17

Location of points

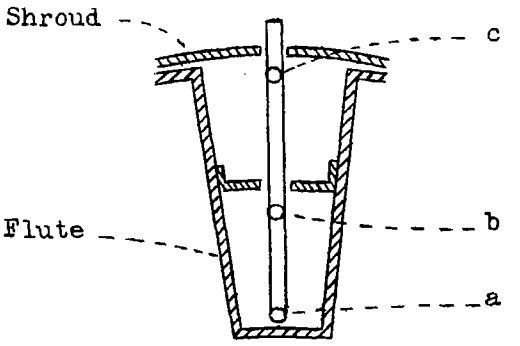

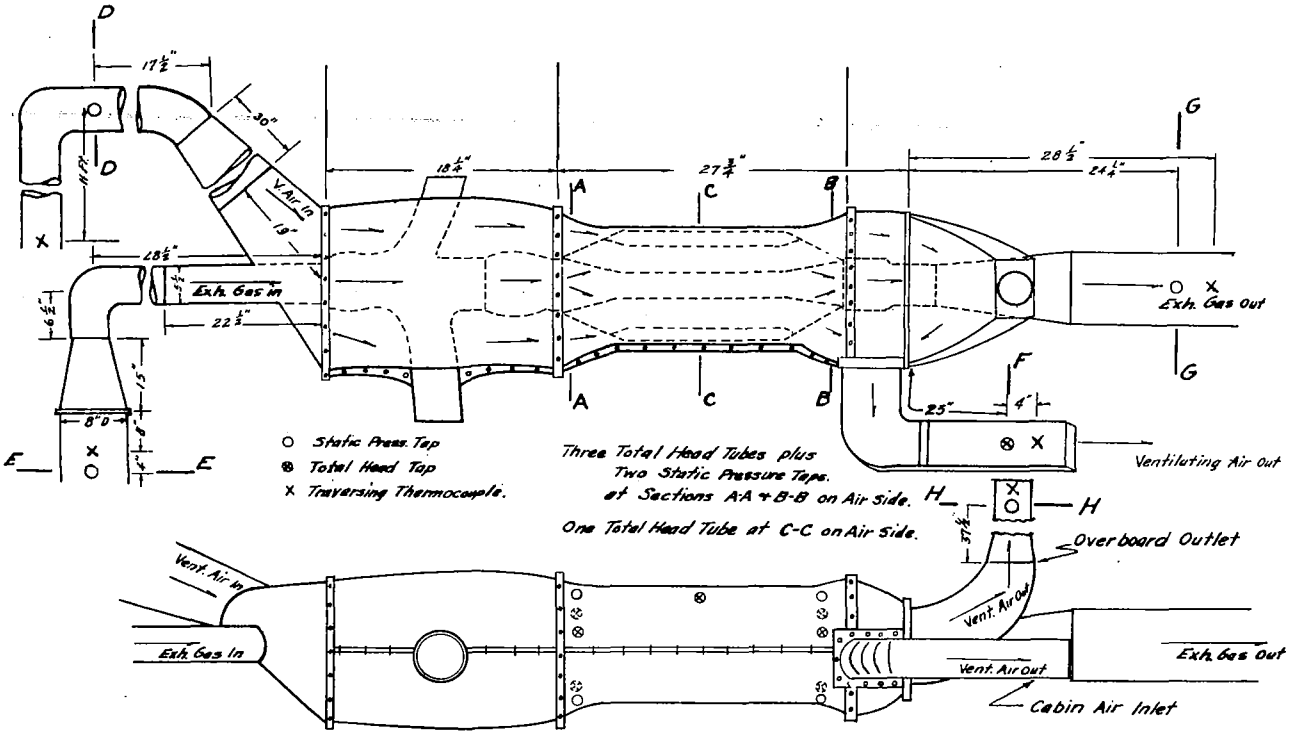

B-3 Shroud

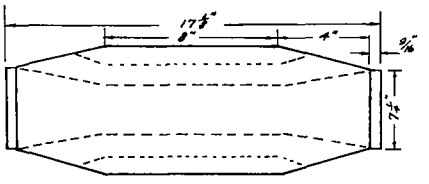

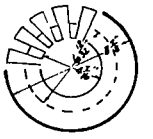

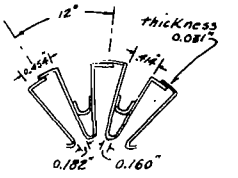

Fluted-Type Heat Exchanger

	APPROACH SECT.		EXIT SECT.		HEAT EXCHANGER SECTION							
	Air Side	Gas Side	Air Side	Gas Side	AIR SIDE				GAS SIDE			
	Weighted Mean Values		Weighted Mean Values		Sect. AA	Sect. BB	Sect. CC	Weighted Mean	Sect. AA	Sect. BB	Sect. CC	Weighted Mean
Cross Sectional Area Ft.²	0.254	0.217	0.400	0.230	0.278	0.321	0.164	0.202	0.287	0.287	0.257	0.265
Wetted Perimeter Ft.	4.58	1.65	4.97	1.70				13.3				9.50
Hydraulic Diameter Ft	0.222	0.526	0.322	0.541				0.0605				0.112
Heat Transfer Area Ft.²	3.87	3.87	3.12	3.12				16.0				13.5

Fig. 1 - Schematic Diagram of Fluted-Type Heat Exchanger and Parallel Air Flow Shroud

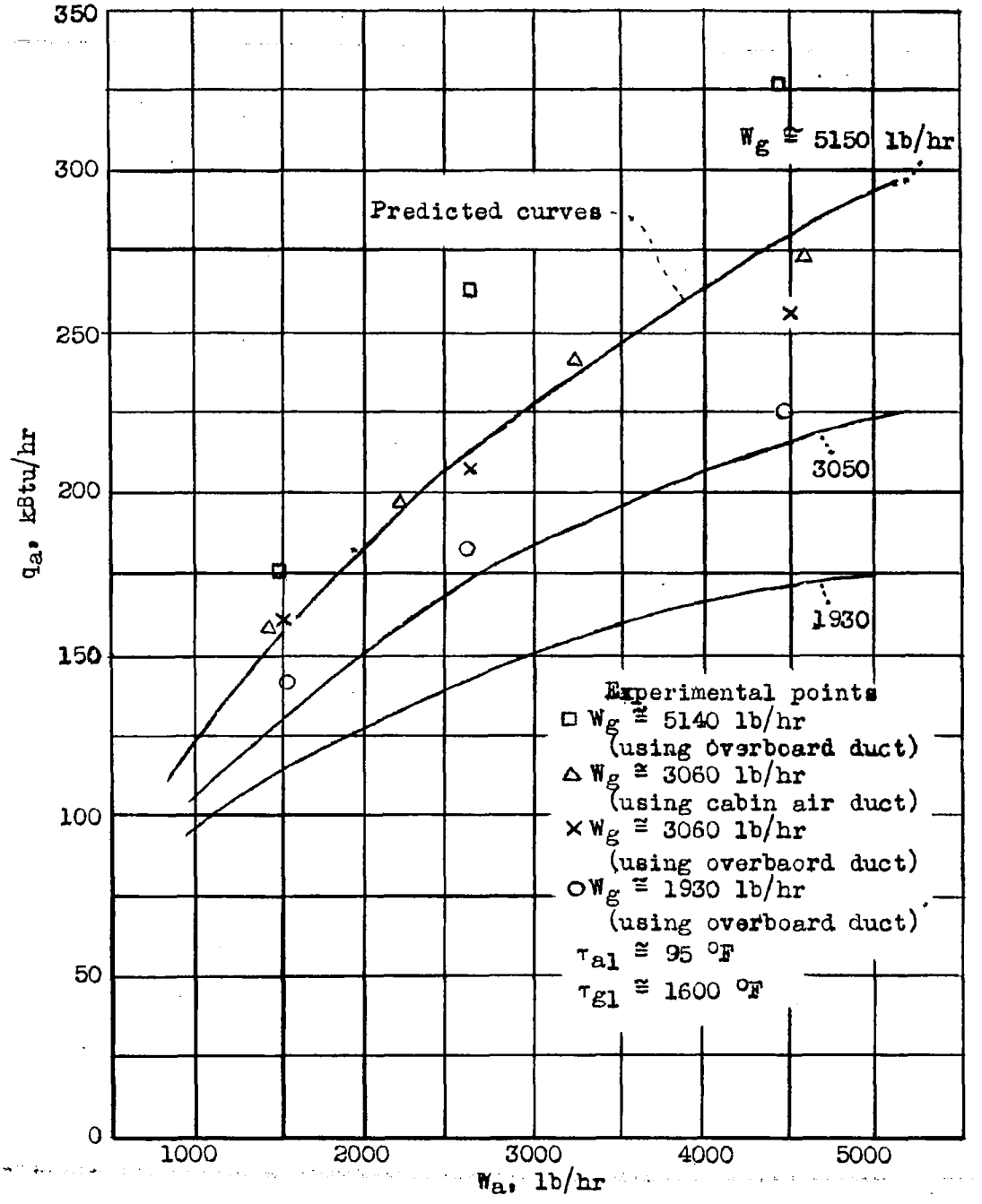

Figure 2.- Thermal output of flattened type heat exchanger using parallel air flow shroud, as a function of ventilating air rate.

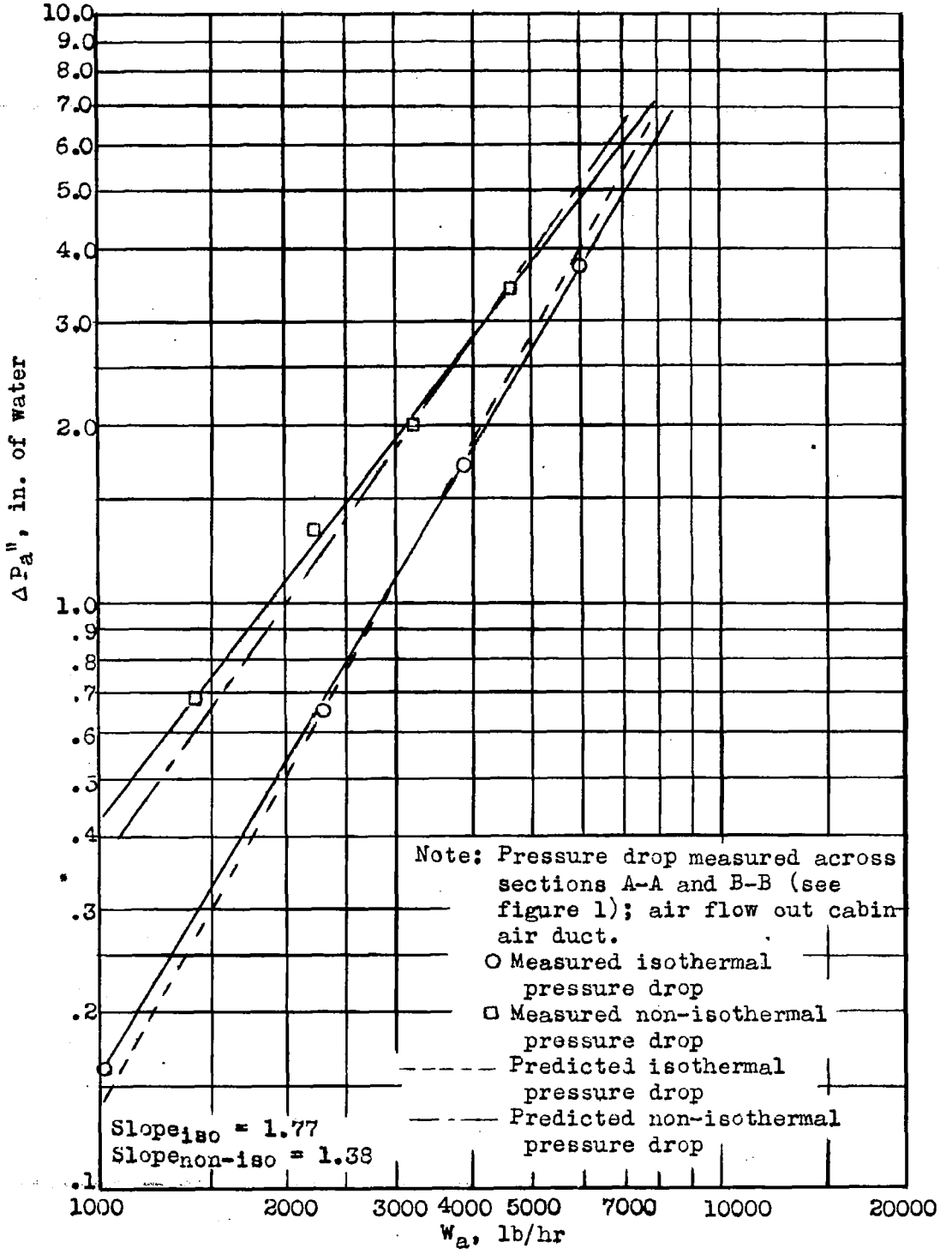

Figure 3.- Static pressure drop across air side of fluted-type heat exchanger, using parallel air flow shroud, as a function of ventilating air rate.

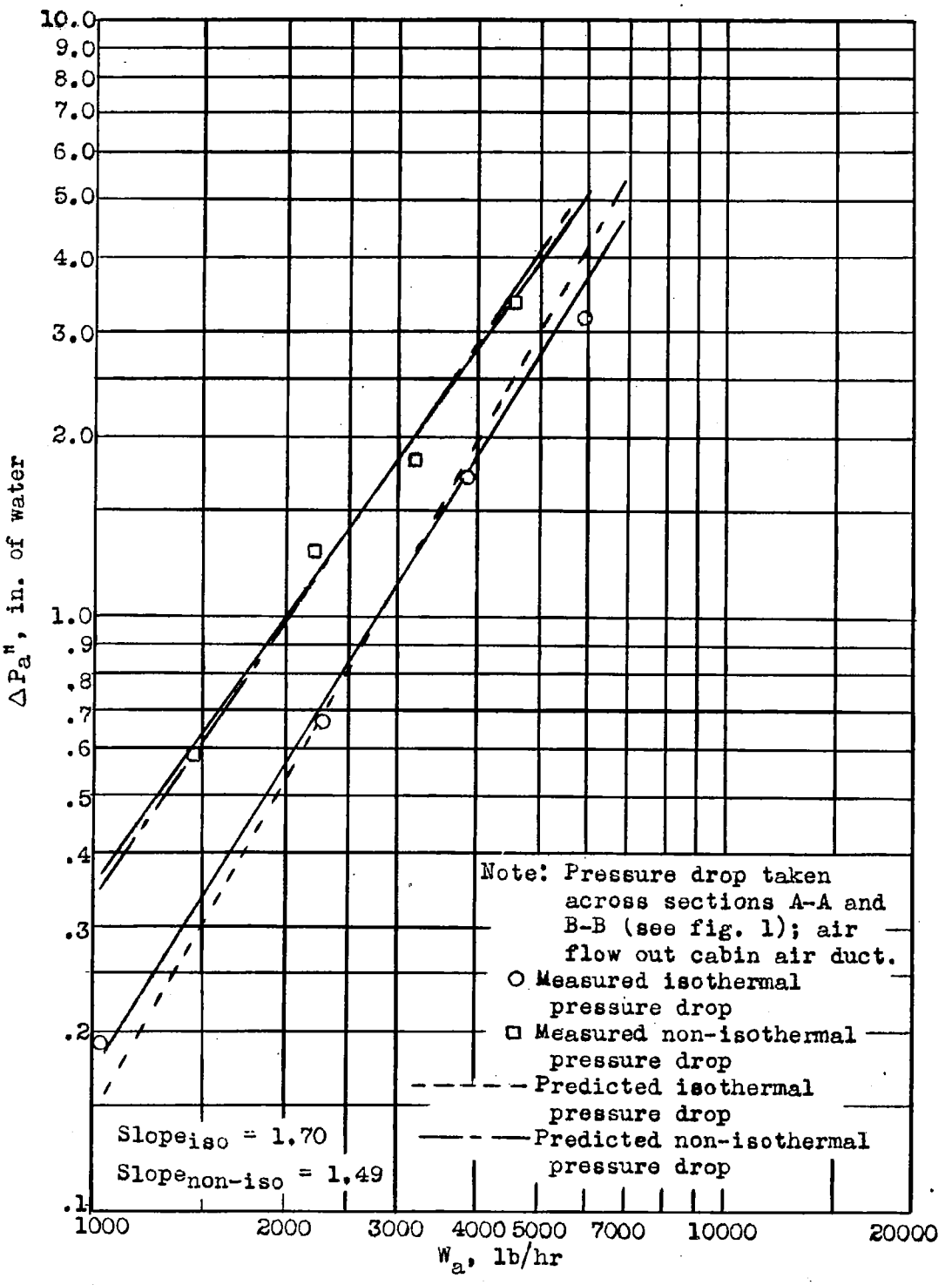

Figure 4.- Total pressure drop across air side of fluted-type heat exchanger, using parallel air flow shroud, as a function of ventilating air rate.

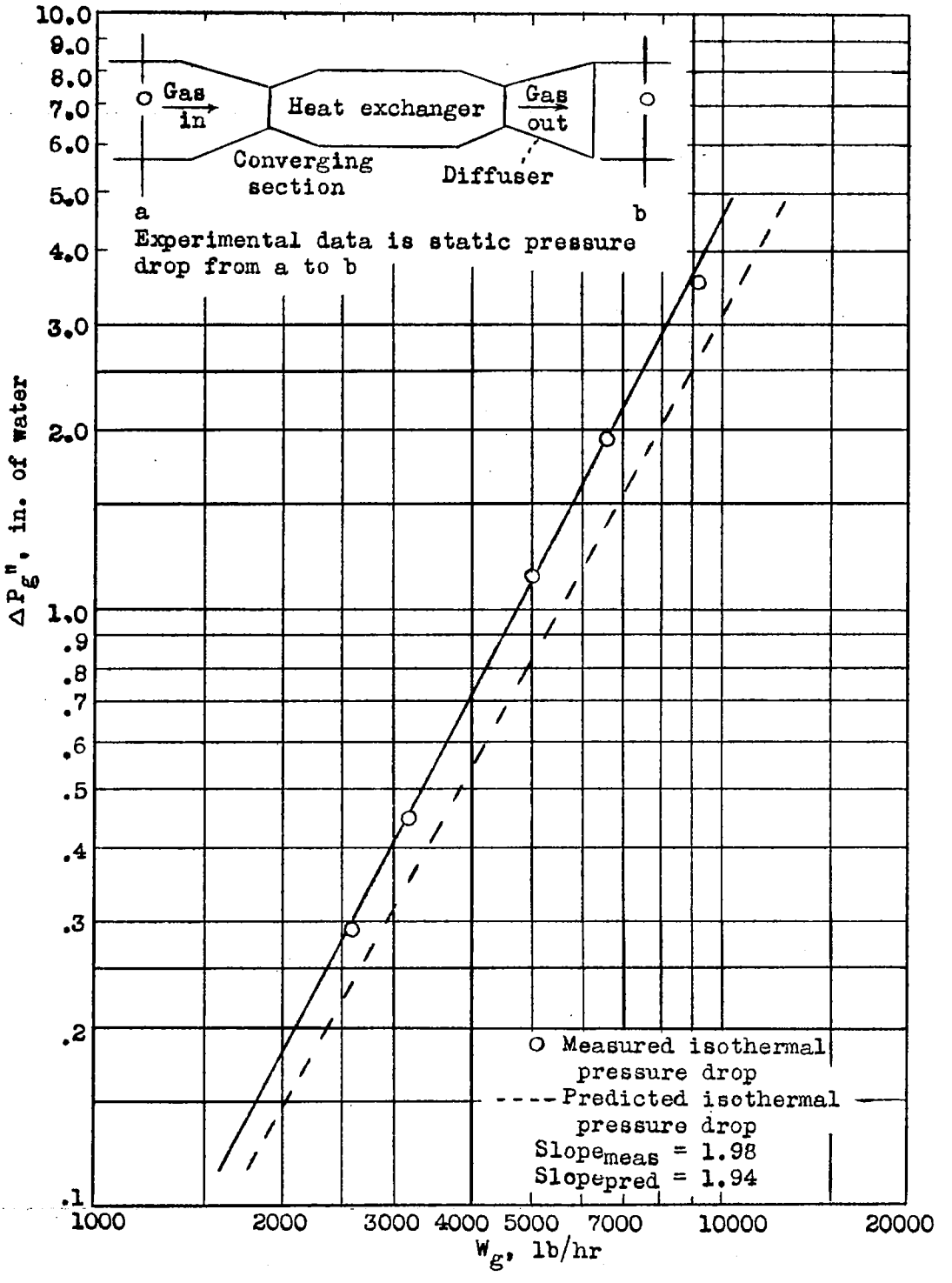

Figure 5.- Static pressure drop across exhaust gas side of fluted-type heat exchanger, with additional reducer and diffuser sections, as a function of exhaust gas rate.

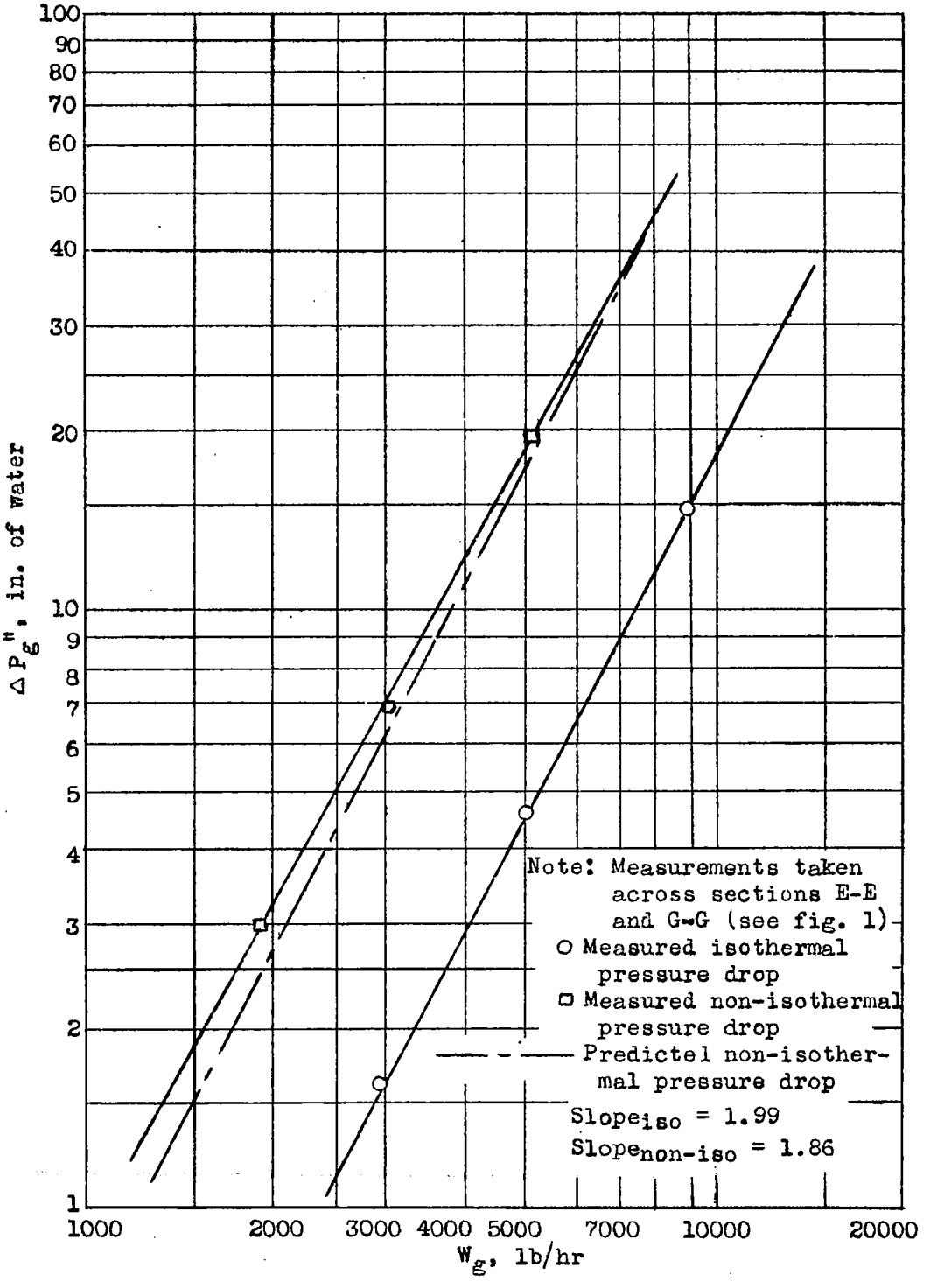

Figure 6.- Overall static pressure drop across the exhaust gas side of the experimental setup, as a function of the exhaust gas rate.

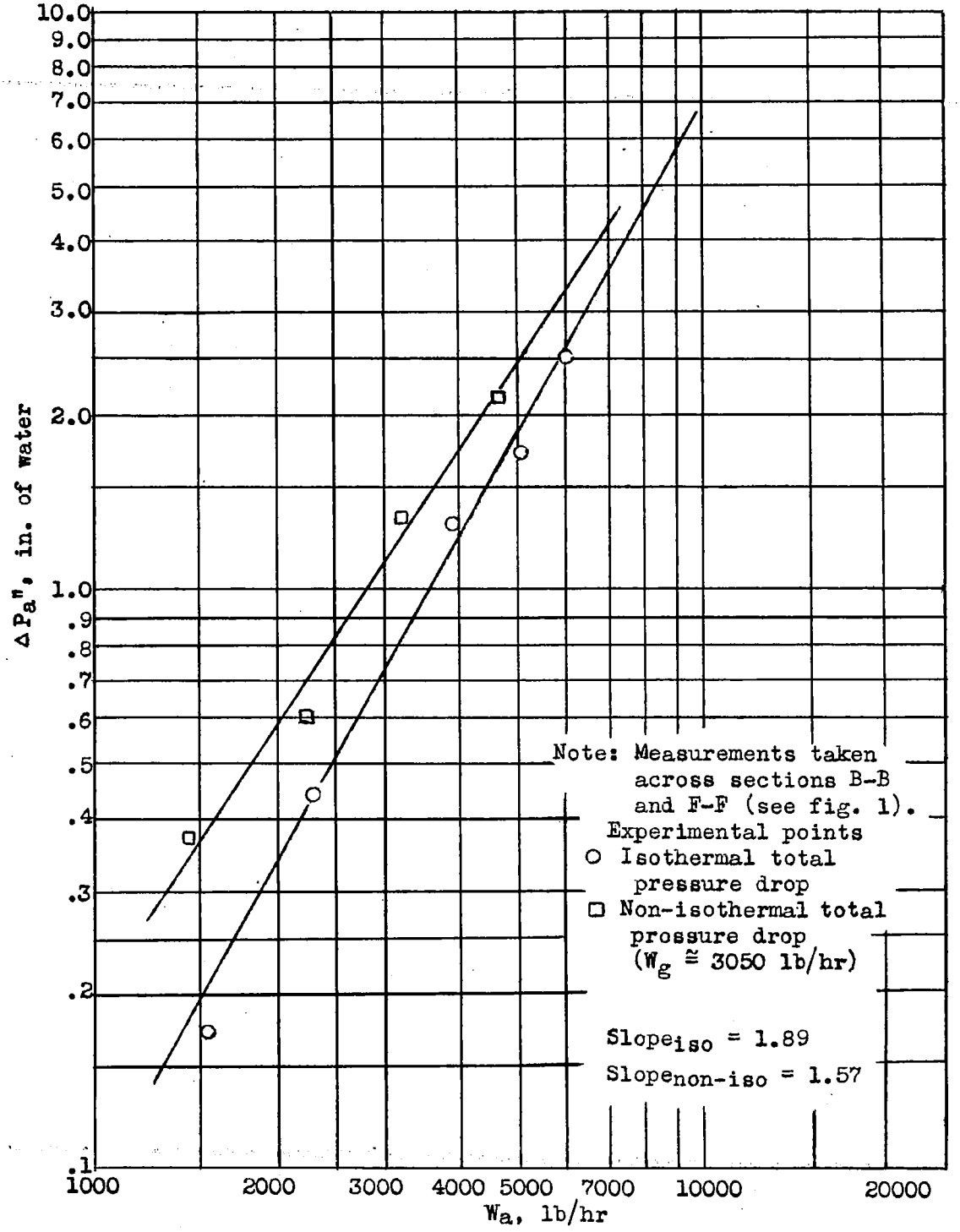

Figure 7.- Total pressure drop across cabin air duct elbow, as a function of ventilating air rate.

ΔP_{htr} isothermal static pressure drop across the heater passages only, lb/ft^2 ($\Delta P'_{htr}$ = inches H_2O)

ΔP_{iso} total isothermal static pressure drop across heater and ducts at temperature T_{iso}, lb/ft^2 ($\Delta P'_{iso}$ = inches H_2O)

ζ isothermal friction factor defined by the equation

$$\frac{\Delta P}{\gamma} = \zeta \frac{l}{D} \frac{u_m^2}{2g}$$

Δt_{mx} mean temperature difference for crossflow as defined by equation (43) of reference 2, $^{\circ}F$

μ viscosity of fluid, lb sec/ft^2

T_{a_1} mixed-mean temperature of ventilating air at entrance section (point 1), $^{\circ}F$

T_{a_2} mixed-mean temperature of ventilating air at exit section (point 2), $^{\circ}F$

T_{g_1} mixed-mean temperature of exhaust gas at entrance section (point 1), $^{\circ}F$

T_{g_2} mixed-mean temperature of exhaust gas at exit section (point 2), $^{\circ}F$

φ_x heater effectiveness for crossflow used in equation (46) of reference 2

Re Reynolds number = $GD/3600 \mu g$

Subscripts

a ventilating-air side

c convective conductance

cs cross-sectional areas

e "effective" thermal conductances

g exhaust-gas side

h, htr heater